MICROSTRUCTURE OF RAPIDLY SOLIDIFIED POWDERS

R. D. Field, A. R. Cox,* and H. L. Fraser**
Department of Metallurgical and Mining Engineering
University of Illinois
Urbana, Illinois 61801

Individual rapidly solidified Ni-based powder particles have been studied in the transmission electron microscope (TEM) in the conventional (CTEM) and scanning (STEM) modes of operation. Information on morphology and microchemistry has been obtained and is related to solidifying conditions.

INTRODUCTION

One of the new techniques for the processing of superalloys which has been explored with increasing enthusiasm in the past decade is the use of rapidly solidified powders in the fabrication of superalloy components. The goal of the present study is to characterize rapidly solidified Ni-based powders in terms of microstructure and associated microchemistry and to relate these observations back to the solidifying conditions.

In order to study these powders on a scale appropriate to their fine microstructures it is necessary to resort to the transmission electron microscope (TEM). Therefore, one must have a technique for the preparation of thinned samples of small particles. Such a technique was developed and, using TEM in the conventional (CTEM) and scanning (STEM) modes, morphological, structural, and chemical observations were made on a very fine scale. In this paper, experimental results will be presented for Ni-based alloy powders produced by rapid solidification.

---

*Government Products Division, United Technologies, West Palm Beach, FL 33402
**Now at UTRC, Silver Lane, East Hartford, CT 06108

EXPERIMENTAL PROCEDURE

The Ni-based superalloy powders for this study were supplied by the Pratt and Whitney Aircraft Government Products Division in West Palm Beach, Florida. They were produced by rotating disk atomization and helium quenching. The powders discussed in this paper are of a Ni-based 14ω/o Mo, 6.0ω/o Ta, 5.8ω/o Al alloy.

Thin foils suitable for transmission electron microscopy were produced using a specially devised technique (1). By electroplating a nickel binder on either side of a layer of powders and subsequently thinning the resultant composite foil using conventional techniques it was possible to produce suitably thinned particles.

A secondary electron image of a typical thinned powder particle is shown in Fig. 1. The particle is held by the matrix of electroplated nickel binder and several other powder particles can also be seen in the perimeter of the micrograph. Perforation has occurred in the particle and areas adjacent to the hole are sufficiently thinned for CTEM and STEM work (~50-500nm).

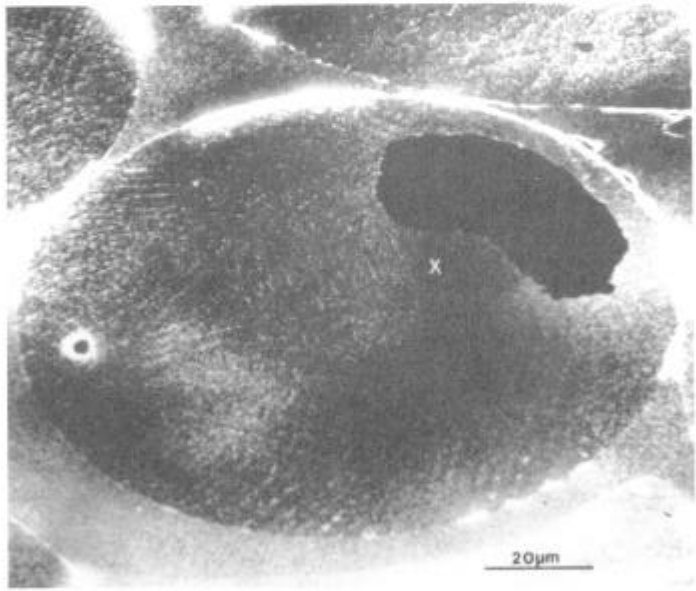

Fig. 1. Secondary electron image of a typical thinned powder particle. Areas adjacent to hole (designated with an "x") are sufficiently thinned for STEM analysis.

RESULTS

Morphological Observations

Three different morphologies were observed in the rapidly solidified powders of several alloys. Results for IN100 and Mar M200 are reported elsewhere (1,2).

The most common morphology was the branched dendritic solidification structure, where both primary and secondary dendrites were observed with growth occurring in the cube directions of the crystal. A second phase was present in the interdendritic regions. The second morphology found had a cellular growth pattern. This differed from the branched dendritic powders in that no secondary dendritic arms were present. Precipitation of an intercellular second phase was also observed in these powders. The third morphology observed had a microcrystalline solidification structure consisting of many individual equiaxed grains with no apparent precipitation in the grain boundaries. The absence of the second phase and the evidence of multiple nucleation sites makes this structure fundamentally different from those in the dendritic and cellular particles.

In Fig. 2 a rare observation of all three of these morphologies in a single powder particle of a Ni-Mo-Ta-Al alloy is shown. Examination of this particle indicates the following

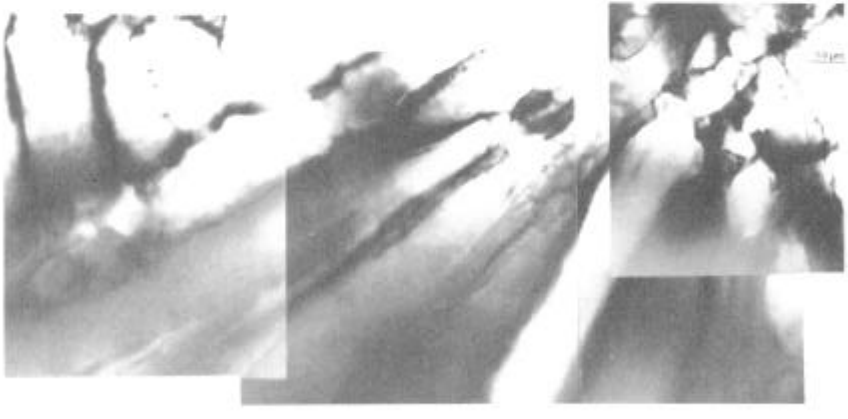

Fig. 2. Transmission electron micrograph of a Ni-Mo-Ta-Al powder particle showing three different morphologies in a single particle.

solidification sequence. Initially several simultaneous nucleation events occurred in the liquid droplet giving rise to the microcrystalline region. This was followed by the development of cellular growth from this area. Further from the initial nucleation region secondary arms evolved growing from the advancing cells. The remainder of the powder solidified in a branched dendritic manner. The mechanisms of these transitions in growth morphology will be examined further in the discussion section.

Microsegregation

In order to further understand the origin of rapidly solidified structures in the powders, microsegregation profiles were measured for the dendritic and microcrystalline powders. The fineness of the microstructure (secondary dendrite arm spacings of approximately 1μm) called for the analytical capabilities of the electron microscope where, in the STEM mode, spatial resolution for elemental analysis by characteristic x-ray emission lines is on the order of 30nm.

In Fig. 3 micrographs from two different Ni-Mo-Ta-Al alloy powder particles are shown. In Fig. 3a, a dendritic morphology is observed with interdendritic precipitation visible. Figure 3b is of a single grain in a microcrystalline specimen. Note that there is no evidence of precipitation in the grain boundaries. In Fig. 4 are shown segregation profiles for the two specimens. These data were obtained by collecting a series of x-ray spectra in the STEM mode from the center of one dendrite arm or grain to the center of the adjacent arm or grain. Severe segregation of Mo and Ta to the interdendritic region has occurred. The Al concentration decreases in the interdendritic region. It is likely that this is caused by the rejection of Al from the second phase as it solidifies. This hypothesis is supported by the slight enrichment of Al adjacent to the interdendritic precipitate.

In the microcrystalline sample segregation of Mo and Ta also occurs during solidification, though not to as great an extent as in the dendritic case. Despite the fact that a concentration gradient from the center of the grain to the grain boundary is observed, second phase precipitation is not evident in the grain boundaries.

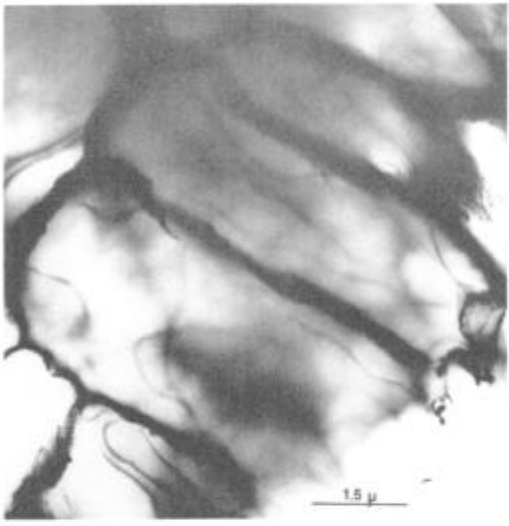

Fig. 3. Transmission electron micrographs of two different powder particles of a Ni-Mo-Ta-Al alloy.
a) dendritic morphology

Fig. 3b. Single grain in a microscrystalline morphology particle

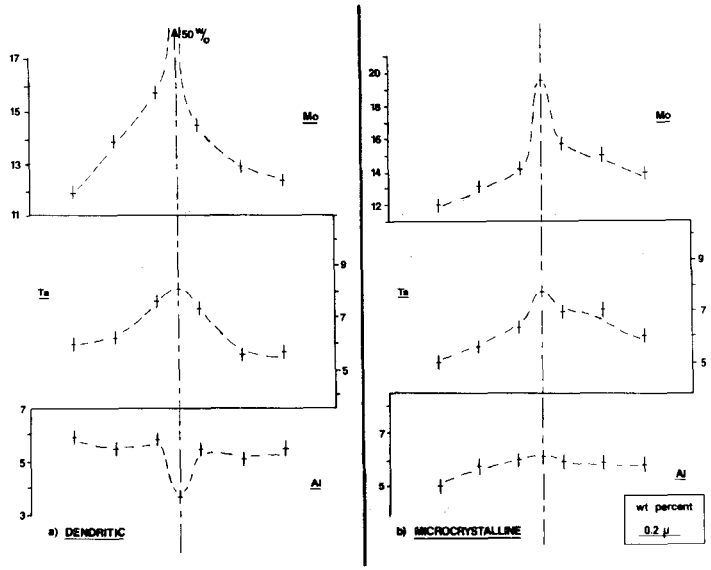

Fig. 4. STEM x-ray data for specimens shown in Fig. 3.
a) dendritic: points taken from center of one secondary dendrite arm to the center of the adjacent arm. Center line indicates interdendritic precipitate.
b) microcrystalline: points taken from center of one grain to center of adjacent grain. Center line indicates grain boundary.

DISCUSSION

The three different solidification morphologies observed in rapidly solidified powders are similar to those reported by Kattamis and his coworkers (3-5) for specimens solidified after various degrees of undercooling of the melt. Kattamis observed a change in nucleation and growth characteristics from branched dendritic to cylindrical(cellular) to spherical (microcrystalline) morphology with increasing undercooling. This suggests that substantial undercooling of the molten powders occurs prior to solidification and that this is responsible for the microstructures observed. Since undercooling is expected to increase with decreasing powder size (6,7) a study of morphologies for various powder size ranges is being preformed.

In the powder shown in Fig. 2, initial undercooling

resulting in a microcrystalline region being formed is decreased as heat of fusion is given off. As the undercooling and solid-liquid interface velocity decrease, the growth morphology changes to cellular and then to branched dendritic.

Segregation in the absence of second phase precipitation in the microcrystalline powders also presents an interesting problem. If local equilibrium at the solid-liquid interface is assumed, composition of the liquid and solid at the interface should follow the solidus and liquidus lines respectively until a second phase is formed. Absence of this precipitation in the grain boundaries suggests that even though heat of fusion given off during solidification raises the temperature of the powder into the two-phase (liquid-solid) region, giving rise to segregation, equilibrium at the interface is not maintained. Solute trapping of the type reported by Cahn (8,9) takes place due to the high velocity of the solid-liquid interface.

Although the microcrystalline morphology clearly is formed by multiple nucleation sites of the solid phase in the liquid powder, it is uncertain whether this is the result of homogeneous nucleation or the activation of a wide spread heterogeneous nucleation agent. According to calculations by Hirth (10) sufficient undercooling for homogeneous nucleation in nickel should be practically unobtainable. However, the author also indicates that these calculations are not reliable since values of parameters used in the equations were not well known.

Kear et al. (11) have also observed what they term microcrystalline structures in powders produced by rotating disk atomization and helium quenching. They explained these structures as resulting from partial solidification on the disk, noting that the occurrence of powders with this morphology decreased with increasing superheat in the melt. In this explanation, the liquid powders have preexisting nuclei picked up from the mushy zone on the disk resulting in a rheocast type structure. Close examination of the structures observed in their study reveal that they are fundamentally different from those termed microcrystalline in the present work. Second phase precipitation is clearly visible in the grain boundaries of the specimens used in their analysis whereas this is not observed in the microcrystalline structures of this study.

CONCLUSION

Some disagreement exists as to whether rapidly solidified

powders are substantially undercooled prior to solidification. In the case of the powders studied in the present work strong evidence for undercooling has been found. Firstly, solidification morphologies identical to those observed in bulk undercooling experiments have been observed. In the case of the microcrystalline morphology, the multiple nucleation events responsible for the structure as well as the single phase nature of the powders strongly indicates extreme undercooling prior to solidification. The substantial difference between the segregation profiles of the microcrystalline and dendritic microstructures coupled with the absence of grain boundary precipitation in the former also suggest fundamentally different solidification mechanisms caused by different undercoolings.

Further studies of a Ni-27^{w}/o Mo binary alloy are in progress in order to further clarify the effects of undercooling and particle size on the solidification morphology and resultant microsegregation characteristics in rapidly solidified powders.

REFERENCES

(1) R. D. Field and H. L. Fraser, Met. Trans, 9A, Jan. 1978, p. 131.

(2) R. D. Field and H. L. Fraser, in Rapid Solidification Processing, Principles and Technologies (Proceedings: International Conference on Rapid Solidification Processing, Preston, VA), Nov. 1977, p. 270.

(3) T. Z. Kattamis and M. C. Flemings, Trans. Met. Soc., 236, Nov. 1966, p. 1523.

(4) T. Z. Kattamis and R. Mehrabian, J. Vac. Sci. Tech., 11, No.6,Nov/Dec. 1974, p. 1118.

(5) T. Z. Kattamis, J. Cryst. Growth, 34, 1976, p. 215.

(6) T. A. Joly and R. Mehrabian, J. Mat. Sci., 9, 1974, p. 1446.

(7) C. Acrivos, J. Mat. Sci., 11, 1976, p. 1752.

(8) J. C. Baker and J. W. Cahn, Acta Met., 17, May 1969, p. 575.

(9) J. C. Baker and J. W. Cahn, in Solidification (ASM), 1971, p. 155.

(10) J. P. Hirth, Met. Trans., 9A, March 1978, p. 401.

(11) B. H. Kear, P. R. Holiday, and A. R. Cox, Met. Trans., 10A, Feb. 1979, p. 191.